Article ID: 1006-8775(2001) 02-0154-09

THE MESOSCALE CONVECTIVE SYSTEMS ACROSS THE TAIWAN STRAIT AND NEIGHBORING AREAS DURING IOP608 OF HUAMEX

ZHENG Yong-guang (郑永光) , WANG Hong-qing (王洪庆), TAO Zu-yu (陶祖钰), WANG Li-qun (王立琨)

(*National Laboratory for Severe Storm Research, Department of Geophysics, Peking University, Beijing,* 100871 *China*)

ABSTRACT: The paper gives the distributions of the daily mean temperature of black body of satellite infrared images from June 7 to 10, 1998 during HUAMEX and examines 14 meso-α-scale convective systems and a number of meso-*b*-scale convective systems using the satellite infrared images at 1-h intervals. The mesoscale convective systems on June 7 and 9, which resulted in severe rainstorm over the middle of Taiwan and the estuary region of the Pearl River (Zhujiang R.), are emphatically analyzed. The serial development of mesoscale convective systems is revealed by the distributions of the black body temperature of satellite infrared images. The environmental conditions in which many mesoscale convective systems continuously occurred are diagnosed. The visualizing tool, LiveView, displays the link between the upper and lower horizontal wind fields and the vertical circulations and 3-dimensional trajectories of moist air motions, based on the data of objective analyses.

Key words: rainstorm; mesoscale convective system; environmental conditions; visualization

CLC number: P458.121.1 **Document code:** A

1 INTRODUCTION

Ever since Maddox[1] put forward the notion of MCC (Mesoscale Convection Complex, a special mesoscale convective system) in the 1980's, much research[2-7] has been documented at home and abroad regarding mesoscale convection systems (MCS). They have been identified as important synoptic systems for causing rainstorms and their life cycle and associated large-scale conditions have been induced and studied through case studies. With the method of composite analysis, Augustine et al.[6] and Zheng[8] discussed the large-scale environmental conditions in which meso-α convective systems (to be simplified as $M_a CS$) occurred.

June 8 ~ 11, 1998 is an intensive observation period (IOP) during a rainstorm experiment across the Taiwan Strait and neighboring areas (HUAMEX). Over the IOP, heavy rain weather occurred in waters off the estuary of Pearl River, Taiwan and Hong Kong. 171 mm of rainfall was recorded in Hong Kong on June 8 alone (Fig.1) and stations with cumulative rainfall amounting over 200 mm in the estuary region the Pearl River include Enping, Zhuhai, Doumen, Boluo, Hong Kong and Macau. Hard rain had been falling in the four days in Taiwan, with the largest rainfall on June 7, which had a maximum 6-h amount up to 357 mm, being the strongest precipitation process in the Taiwan heavy rain experiment for 1998. It is for this reason that we include the situation on June 7 in the analysis of the IOP. Miller et al.[9] and Ma et al.[10] conducted comprehensive surveys of mesoscale convective systems and discovered that the south

---

Received date: 2000-05-15; **revised date:** 2001-08-17
Foundation item: National Scaling 95-special project-03; Natural Science Foundation of China (49735180); Foundation for Visiting Scholars for Higher Education Colleges
Biography: ZHENG Yong-guang (1974 –), male, native from Anqiu County of Shandong Province, Ph.D. candidate, mainly involving in the study of mesoscale meteorology.

of China is one of the regions with frequent occurrence of mesoscale convection. Studying the GMS infrared satellite imageries for June 7 ~ 11, 1998, we have found that the regime causing the rainstorm is a mesoscale convective system. Its definition generally follows that used in reference [10] for the meso-α (called $M_a CS$) and meso-β ($M_b CS$) convective systems but the horizontal scale of the meso-α system have been redefined to be 200 ~ 2000 km and that of the meso-β system to be 20 ~ 200 km.

A comprehensive survey is conducted in the present work to study the mesoscale convective systems using the hourly GMS-5 infrared imagery in addition to studying the evolution of the process from June 7 to 11. To have a close look at the condition with which it generates and develops, the Cressman successive correction is used to have a diagnosis based on objective analysis with the aid of conventional sounding data. For the convenience of concrete computation, the results of objective analysis and diagnosis were incorporated into a visualized system, LiveView[11], developed by the National Laboratory for Severe Storm Research, Department of Geophysics, Peking University. The tool was used to analyze the condition suitable for the generation and development of mesoscale convective systems and some useful results were obtained.

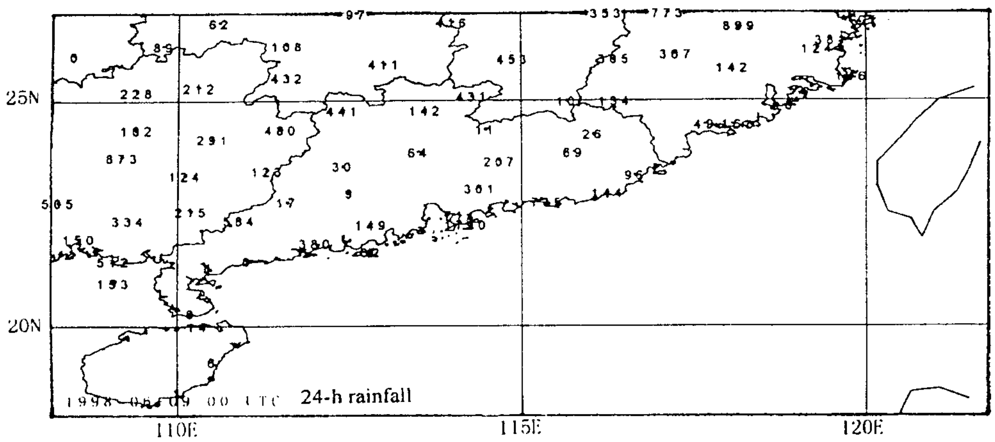

Fig.1 24-h precipitation in southern China (not including Taiwan province) for 0000 UTC June 9, 1998 (unit: 0.1 mm)

2 BASIC CHARACTERISTICS OF CLOUD IMAGERY (DAILY MEAN CLOUD MAPS)

To show the reader a general summary of cloud-cluster activity over the period, we made a daily mean distribution of T_{BB} by the infrared. It is shown in Fig.2 that on June 7 stretches of frontal clouds extended westward from the western Pacific Ocean to the northern part of South China Sea, bringing cloud bands colder than –32°C over waters southeast of the mouth of the Pearl River and southern Taiwan, which was indicating severe activity of MCS in the northeastern South China Sea on the day. By June 8, a frontal cloud band formally active over the Changjiang R. (Yangtze) had made southward displacement to regions near the Nanling Mountains with the westernmost end arriving at the coast of Guangxi. In the meantime, maritime cloud bands had some northward movement with a cold center lower than –52°C at the western edge. The MCS features were strongly displayed. Its northern boundary affected the Pearl River Mouth and waters of Guangdong east of it and brought usually heavy rain to Hong Kong. At the same time, a meso-β cold cloud area concentrated over the Island of Hainan. When it came to

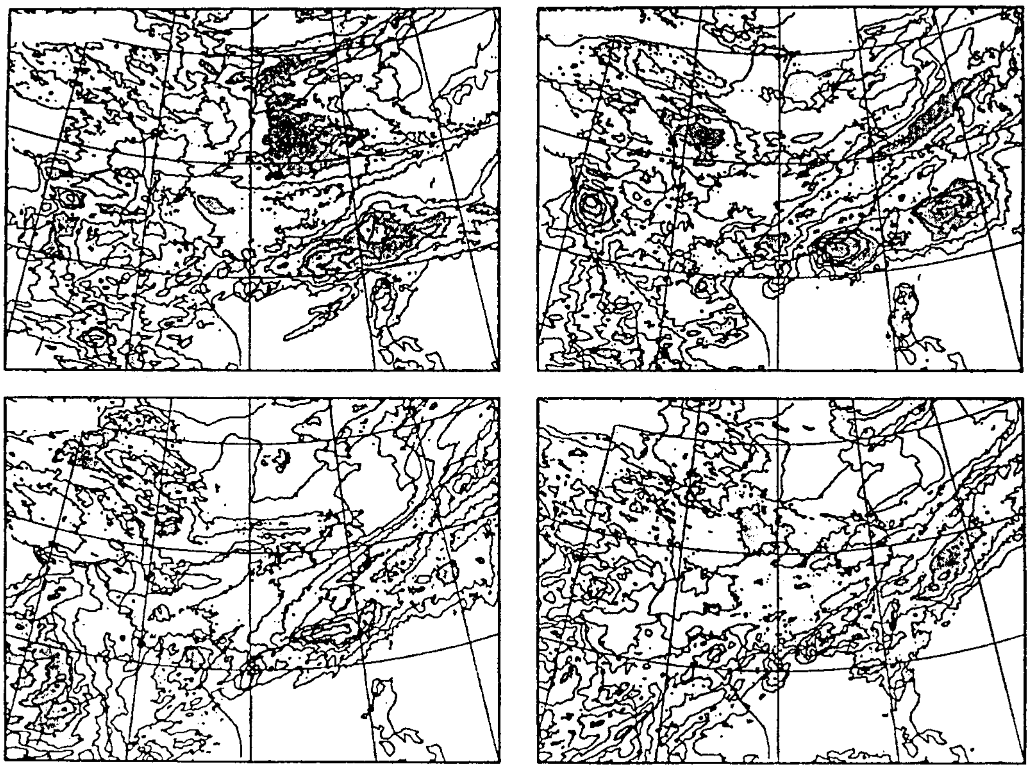

Fig.2 Contours of satellite infrared images with daily mean black body temperature less than –32°C for June 7 ~ 10, 1998

June 9, the frontal cloud bands over the main land traveled to the coast of southern China, coinciding with those over the sea at the western end. T_{BB} was lower than –32°C and –52°C over the waters of eastern Guangdong and southern Taiwan, respectively. By June 10, frontal clouds over the land had moved to the southern China coast while the coverage and intensity of cold cloud bands active along its western section decreased to some extent.

3 ACTIVITY AND EVOLUTION OF MCS

The comprehensive survey with GMS-5 hourly infrared imagery has isolated a total of 14 meso-α convective systems that have T_{BB} colder than –32°C at the cloud veil and horizontal scale larger than 200 km. Tab.1 and Fig.3 give the general summary of the cloud clusters. Among them, six (1, 2, 3, 4, 5, 6, 7#) were generally over the sea for the entire life cycle, five (8, 9, 11, 13, 14#) were near the coast, one (10#) was entirely over the land and the remaining two formed over the Taiwan Strait before moving across Taiwan. All of the cloud clusters were generally heading towards the northeast by east and tended to dissipate 2 ~ 3 hours after the cold veil enlarged to its maximal size. The longer the life cycle, the larger the maximum cold cloud veil would be.

Tab.1 The $M_a CS$ s ($\geq$200 km) and partial $M_b CS$ s (>150 km and <200 km) for June 7 ~ 10, 1998

Serial No.	Onset - dissipation	Formation, max.	Location	Note
1	06 UTC 7th	01 UTC, 03 UTC 7th	Off Pearl R. Mou.	
2	10～20 UTC 7th	15 UTC, 17 UTC 7th	Bashi strat	From remainder of 1#
3	11～22 UTC 7th	17 UTC, 18 UTC 7th	Bashi strat	Same as above
4	10～23 UTC 7th	13 UTC, 17 UTC 7th	Taiwan	Same as above & redevelop
5	18 UTC 7th ～ 04 UTC 8th	22 UTC 7th, 01 UTC 8th	W. GD coast	
6	19 UTC 7th ～08 UTC 8th	01 UTC, 05 UTC 8th	NE. SCS	
7	05 UTC 8th ～00 UTC 9th	12 UTC, 18 UTC 8th	E. GD coast	From remainder of 5#
8	16 UTC 8th ～05 UTC 9th	21 UTC 8th, 02 UTC 9th	Pearl R. Mouth	Redevelop
9	11 UTC 8th ～00 UTC 9th	17 UTC, 22 UTC 8th	Coastal Beibu Bay	
10	06 ～15 UTC 8th	12 UTC, 13 UTC 8th	Guangxi	
11	05 ～14 UTC 9th	09 UTC, 12 UTC 9th	E. GD	From *b*2
12	14 UTC 9th ～01 UTC 10th	16 UTC, 18 UTC 9th	S. Taiwan Strait	From remainder of 11#
13	04 UTC～12 UTC 10th	08 UTC, 10 UTC 10th	W. GD	
14	18 UTC 10th	21 UTC, 23 UTC 10th	Pearl R. Mouth	
*b*1	18 UTC 8th ～02 UTC 9th	23 UTC 8th	Guangxi	
*b*2	22 UTC 8th ～03 UTC 9th	00 UTC 9th	W. GD	
*b*3	06 UTC ～12 UTC 9th	10 UTC 8th	Hainan	
*b*4	08 UTC ～16 UTC 9th	12 UTC 9th	Hainan	
*b*5	20 UTC 9th ～10 UTC 10th	01 UTC, 06 UTC 10th	Pearl R. Mouth	Split to two & affect E.GD
*b*6	18 ～23 UTC 10th	20 UTC 10th	Hainan	

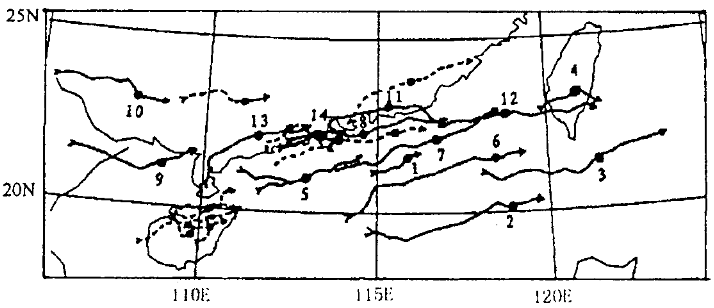

Fig.3 Comprehensive survey results of MCSs for June 7 ~ 10, 1998 (Solid lines: tracks of $M_a CS$ from initial convection to dissipation; dashed lines: same as the solid lines but for $M_b CS$; black dots: positions at the time of maximum extent)

To show the evolution of $M_a CS$, Fig.4 gives the distribution and evolution of $M_a CS$ T_{BB} that brought heavy rain to Guangdong and Taiwan on June 7 and 9. At 0300 ~ 2000 UTC June 7, four $M_a CS$ (1~ 4#) appeared near Taiwan and the Bashi Strait. In the morning of June 7 (0100 UTC, figure omitted), a convection system evolved into a $M_a CS$ (1#) in waters of northern South China Sea off the eastern Guangdong coast but weakened after 0300 UTC. The decreased $M_a CS$ and convective cells nearby gradually evolved into multiple cloud clusters on smaller scale, forming a group of spirally structured convective activity (0700 UTC) which related with the other three $M_a CS$. Moving eastward, the spiral convection zone came near Taiwan by the northern convective band at 1100 UTC when a convective cell developed rapidly off the southwest coast of the island. By 1300 UTC, a $M_a CS$ (4#) covered the southern part of Taiwan. By 1700 UTC, its –63°C cold veil enveloped central Taiwan and moved east over sea around

2000 UTC. Due to the fact that a fresh convective cell was growing rapidly at 1700 UTC off the southwestern Taiwan, a –63°C cold veil again got hold of central and southern parts of Taiwan at 2000 UTC and brought about abundant amount of precipitation. At 1100 UTC, two of the convective cells redeveloped over sea in the spiral-shaped convection area because of radiation cooling at cloud top, acquiring the intensity of $M_a CS$ respectively at 1500 and 1700 UTC (2# and 3#). These maritime $M_a CS$ posed no influence on Guangdong and Taiwan (Fig.3).

Fig.4 gives evolution of the 11# and 12# $M_a CS$ on June 9. They developed in the spiral-shaped convection zone left over as a result of the weakened 9# $M_a CS$ on the 8th day of the month. The figure shows that a convective system on the β scale was growing vigorously over land east of the estuary of the Pearl River in the afternoon (0600 UTC) and intensified to be a $M_a CS$, with half of its cold veil over land and the other half over sea, bringing heavy rain to the coast of eastern Guangdong. At the same, a convective cell to the northwest rapidly developed and merged into it, gaining a maximal cold cloud veil at 1200 UTC. Afterwards, two

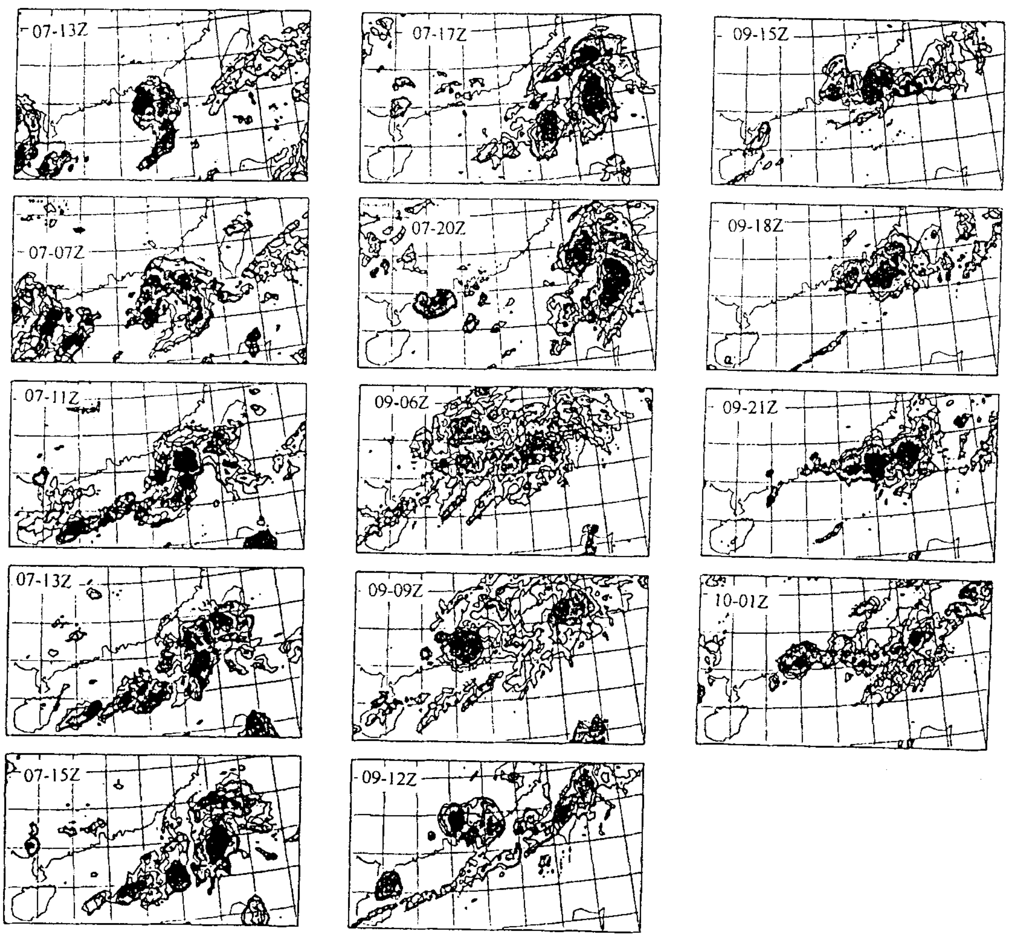

Fig.4 Contours of satellite infrared images with black body temperature less than –32°C for 0300, 0700, 1100, 1300, 1500, 1700, 2000 UTC, June 7, 0600, 0900, 1200, 1500, 1800, 2100 UTC, June 9, and 0100 UTC June 10 (intervals: 10°C)

of cold centers from the $M_a CS$ reorganized into two $M_b CS$. After the splitting, the system weakened significantly in the western section while developed again in the eastern one starting from 1500 UTC. It reached the strongest period at 1800 UTC and became a $M_a CS$ (12#). It did not have any effect on the province of Guangdong since it was active over the sea. It began decreasing at time after 1900 UTC, though being felt in the southern part of Taiwan in the eastward movement. The 11# and 12# $M_a CS$ can be viewed as a single system that has two periods of development in the life cycle. During the evolution of 12# $M_a CS$, three more convective systems were also developing on scales slightly less than the meso-α criterion.

4 CONDITIONS OF LARGE-SCALE ENVIRONMENT AND VISUALIZATION

As in the past research on heavy rain[12-14], we have also found that appearance of heavy rain period during IOP 608 is related not only with the southwest monsoon but with shallow and transformed cold air returning over the sea from the planetary boundary layer (925 hPa). On June 7, a MCS took place just at the eastern end of the 850-hPa southwest monsoon, corresponding to a region of returning easterly flow in the boundary layer. From Fig.5, it is clear that the 925-hPa easterly and 850-hPa southerly on June 7 contributed to significant clockwise turning of

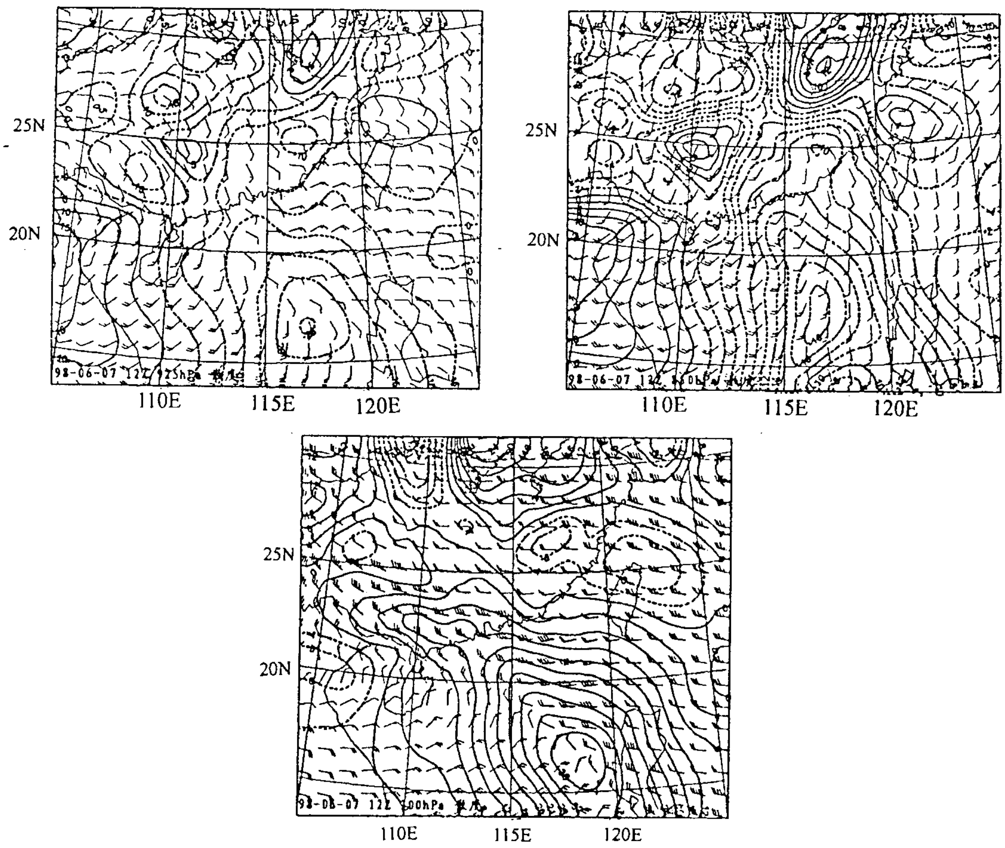

Fig.5 Fields of wind and divergence for 925 hPa, 850 hPa and 200 hPa at 1200 UTC June 7 (unit of divergence: $10^{-6} s^{-1}$)

low-level wind field with altitude in the northeastern South China Sea, which was a typical vertical structured flow field favorable for the generation and development of MCS. The area was of significant convergence as indicated in a study of low-level field. Additional wind field study showed that there was obvious divergence field in the upper level of troposphere over the northeastern South China Sea. It was associated with the downstream increase of wind speed at the inlet of a westerly jet stream for the upper-level tropical subtropical high and the clockwise turning of a westerly to an easterly in the eastern end of the subtropical high ridge in South Asia. Our 5-dimensional visualizing system LiveView[12] clearly shows the linkage between MCS and the three air flows obtained by objective analysis based on observations. In Fig.6, the MCS in the northeastern South China Sea is represented by an equiscalar surface with vertical velocity of 7.3 cm/s, in which the 12-h trajectory indicates how updraft are affected by the three air flows to migrate to the MCS.

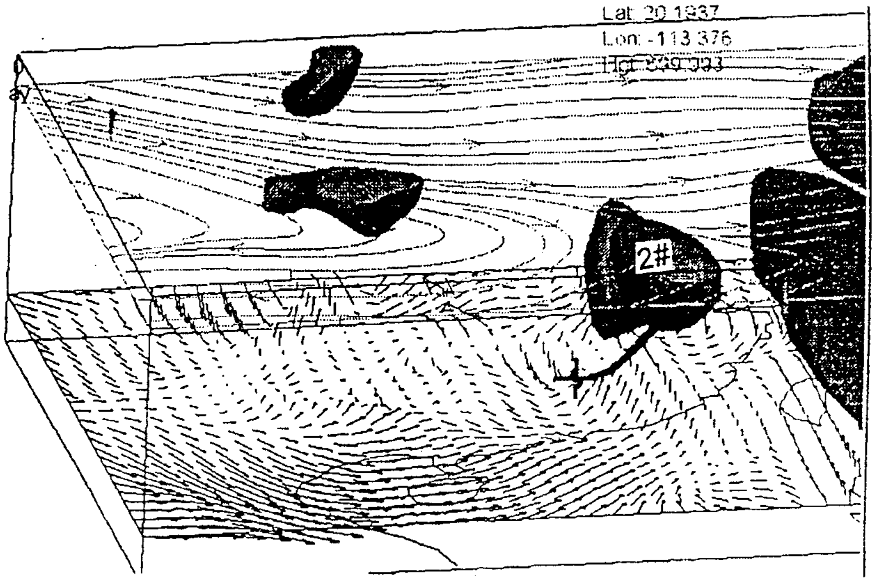

Fig.6 Three-dimensional stream field structure (of equiscalar surface with vertical velocity of 7.3 m/s, 200-hPa stream line and 850-hPa wind field, numerals in the figure represent corresponding MCSs), 12-h air-parcel trajectory (belt-shaped curves), at 1200 UTC June 7

The southwest monsoon took control of the entire region of northeastern South China Sea beginning from June 8, leaving the easterly return flow nowhere to find at 950 hPa. It is interesting to note that in the 3-dimensional distribution of ascending flow zone at 0000 UTO on June 9 as indicated by the LiveView (Fig.7), five mesoscale updrafts over Vietnam, Hainan Is., outer area of the Pearl River Mouth and waters east of the Taiwan Strait and the island itself were aligned into a line, largely corresponding to a number of low T_{BB} zones in the mean distribution for the day. It appeared that these ascending air currents were reflecting the MCS that successively showed up on June 9. As shown in the figure, stream lines flowing in the northeast-southwest vertical profile across the river estuary demonstrate the low-level convergence and rise of southerly and northerly flows over areas where there were MCS and outflow in the upper-level westerly. The 48-h trajectories (figure not shown) indicate that moisture for the MCS in the northeastern South China Sea originated from the Indo-china Pen. and southern South China Sea.

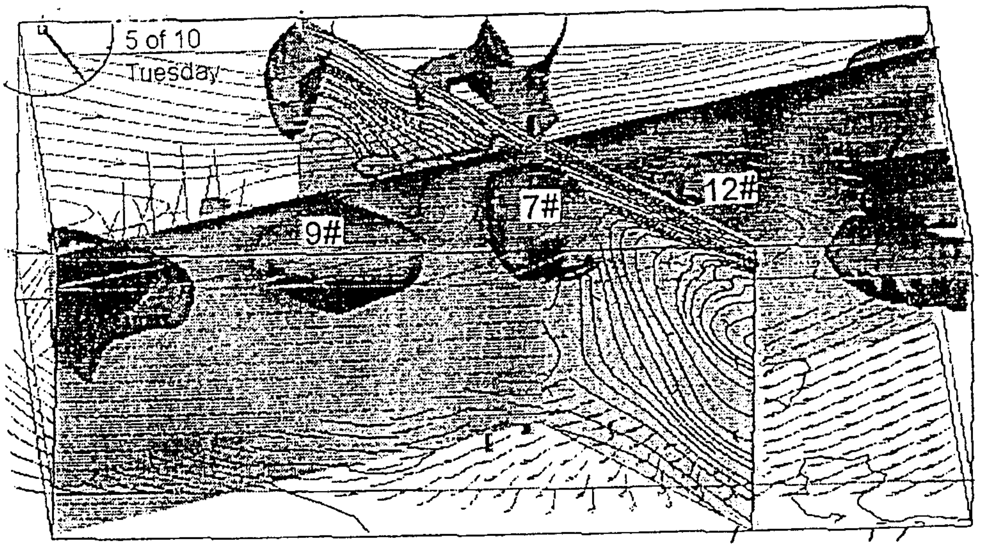

Fig.7 Three-dimensional stream field structure (of equiscalar surface with vertical velocity of 7.3 m/s, stream lines at 200 hPa and vertical profile and wind vector at 925 hPa, numerals in the figure represent corresponding MCSs) at 0000 UTC June 9

Examining the objective analysis data of IOP608 using the LiveView, we found that on June 7 the returning maritime easterly flow carried a much thinner layer of moist air than the southwest monsoon (figure not given). It is more interesting to note that the equiscalar surface of 346-K potential equivalent temperature has a tube-like structure connecting the upper and lower portions of the troposphere (figure omitted), which seems to display the wet adiabatic process within the MCS. A more thorough revelation of the interior structure and evolutionary cycle of MCS can be possible only with numerical model output by LiveView, which is highly resolved in both time and space.

5 CONCLUSIONS AND DISCUSSIONS

a. By studying the hourly GMS-5 infrared cloud imagery, we have shown the evolution of mesoscale convective systems in continuous generation and development during the IOP608.

b. The visualizing tool, LiveView, is used to display the 3-dimensional flow field that favors the generation and development of mesoscale convective systems during the IOP608, with the discovery that moisture needed in the growth originate from the Indo-china Pen. and southern South China Sea.

c. With the aid of LiveView, a tube-shaped structure is found on the equiscalar surface of 346-K potential equivalent temperature that connects the upper tropospheric layers with the lower ones. The finding remains to be verified by studying relevant numerical simulations with high resolution in future.

Acknowledgements: Mr. CAO Chao-xiong, who works at the Guangzhou Institute of Tropical and Oceanic Meteorology, has translated the paper into English.

REFERENCES:

[1] MADDOXR A. Mesoscale convective complexes [J]. *Bulletin of American Meteorological Society*, 1980, **61**: 1374-1387.

[2] FANG Zong-yi. The preliminary study of medium-scale cloud clusters on Changjiang basin in summer [J]. *Advances in Atmospheric Sciences*, 1986, **2** (3): 334-340.
[3] LI Yu-lan, WANG Jing-rong, ZHENG Xin-jiang, et al. The study on the mesoscale convective complex (MCC) over the Southwest and South of China [J]. *Scientia Atmospherica Sinica*, 1989, **13** (4): 417-422.
[4] XIANG Xu-kang, JIANG Ji-xi. Mesoscale convective complexes over the southern China mainland [J]. *Quarterly Journal of Applied Meteorology*, 1995, **6** (11): 9-17.
[5] JIANG Ji-xi, YE Hui-ming. A study on meso-α convective cloud cluster in southern China [J]. *Journal of Chinese Meteorological Science Academy*, 1986, **1** (2): 132-141.
[6] AUGUSTINE J A, HOWARD K W. Mesoscale convective complexes over United States during 1986 and 1987 [J]. *Monthly Weather Review*, 1991, **119**: 1575-1589.
[7] STANLEY B T, DAVID B P, Evolution of environmental conditions preceding the development of a nocturnal mesoscale convective complex [J]. *Monthly Weather Review*, 1991, **121**: 1078-1098.
[8] ZHENG Y G, TAO Z Y, WANG H Q, et al. Environment of meso-α- scale convective system development in Yellow Sea region [J]. *Progress in Natural Science*, 1999, **9** (11): 842-848.
[9] MILLER D, FRITSCH J M. Mesoscale convective complexes in the western Pacific region [J]. *Monthly Weather Review*, **119**: 2978-2992.
[10] MA Y, WANG X, TAO Z Y. Geographic distribution and life cycle of mesoscale convective system in China and vicinity [J]. *Progress in Natural Science*, 1999, **7** (6): 701-706.
[11] WANG Hong-qing, ZHANG Yan, TAO Zu-yu, et al. Multi-dimensional data sets visualization in meteorology [J]. *Progress in Natural Science*, 1998, **8** (6): 742-748.
[12] SUN Shu-qing, ZHAI Guo-qing. Relationship between easterly jet stream and heavy rains within the boundary layer north of the shear line [J]. *Journal of Hangzhou University*, 1983, **10** (1): 119-126.
[13] LI Jian-hui, ZHANG Dong-hua, YANG Ding-qi. Relationship between coastal fronts and heavy rains in the South China's early rainy period [J]. *Acta Meteorologica Sinica*, 1984, **42** (3): 370-374.
[14] ZHAI Guo-qing, SUN Shu-qing. The structure of local boundary layer wind field and strong convective weather [J]. *Meteorological Monthly*, 1986, **12**(11): 6-8.